Structural Engineering and Mechanics, Vol. 17, No. 6 (2004) 829-862
DOI: http://dx.doi.org/10.12989/sem.2004.17.6.829

Nonlinear analysis of reinforced concrete beam elements subject to cyclical combined actions of torsion, biaxial flexure and axial forces

Gian Michele Cocchi† and Paolo Tiriaca‡

Università di Ancona, Facoltà di Ingegneria, Istituto di Scienza e Tecnica delle Costruzioni, Ancona 60131, Italy

(Received September 17, 2002, Accepted October 1, 2003)

Abstract. This paper presents a method for the nonlinear analysis of beam elements subjected to the cyclical combined actions of torsion, biaxial flexure and axial forces based on an extension of the disturbed compression field (DSFM). The theoretical model is based on a hybrid formulation between the full rotation of the cracks model and the fixed direction of the cracking model. The described formulation, which treats cracked concrete as an orthotropic material, includes a new approach for the evaluation of the re-orientation of both the compression field and the deformation field by removing the restriction of their coincidence. A new equation of congruence permits evaluating the deformation of the middle line. The problem consists in the solution of coupled nonlinear simultaneous equations expressing equilibrium, congruence and the constitutive laws. The proposed method makes it possible to determine the deformations of the beam element according to the external stresses applied.

Key words: cyclic loads; reinforced concrete; cracking (fracturing); spatial truss; stress-strain relationships; aggregate interlock; equilibrium; congruence; Mohr's circle; numerical analysis.

1. Introduction

The capacity to simulate structural behaviour under cyclical loading conditions is presently being developed. The model proposed in this paper permits analysing the behaviour of reinforced concrete beam elements subjected to cyclical loads. The most recent truss-like model treats the cracked reinforced concrete elements as an orthotropic material. The interaction relation between flexure, torsion and shear were developed by Elfgren (1972). Compatibility conditions of reinforced concrete elements subjected to shear were introduced by Collins (1973). A fundamental contribution in understanding shear behaviour was given by the discovery of softening in concrete struts in model produced by Robinson and Demorieux (1968) and the first quantification of the phenomenon was given by Vecchio and Collins (1981, 1982).

The nonlinear analysis of FEM of a reinforced concrete element subjected to cyclical actions (Bahn and Hsu 2000) was developed following the model with a rotation of the cracking angle and

† Associate Professor in Structural Engineering
‡ Research Assistant

the model with a fixed cracking angle. The first is based on the gradual re-orientation of the direction of cracking compatibly with the load applied and with the response of the materials. Examples of such formulations come from Foster (1992), Ayoub and Filippou (1998), Barzegar-Jamshidi and Schnobrich (1986). On the contrary, in the second model, the direction of cracking coincides with that of original cracking and remains unvaried. An important aspect of the model with a fixed angle of cracking, proposed by Okamura and Maekawa (1991), Kaufmann and Marti (1998) and others, is the evaluation of the relative slippage which develops between the fracture surfaces and the shear tensions due to the aggregate interlock phenomenon and in the presence of reinforcements which prevent widening of the cracks. The model with a fixed angle of cracking, with cracks oriented in the direction of the compression stresses, was proposed for the nonlinear analysis of the membrane elements in reinforced concrete by Pang and Hsu (1996).

A general calculation method was described by Collins *et al*. (1996) thus simplifying the theory of the modified compression field (MCFT); various nonlinear procedures involving the FEM have been developed by Vecchio *et al*. (1996).

The difficulty, related to the theory of the modified compression field (MCFT), is represented by the control of the shear tensions between the fracture surfaces in that normal tensions may give a non null value of these (Vecchio and Collins 1986). The compatibility equations of MCFT do not take into consideration the slippage due to the shear along the fracture surface. The disturbed strain field theory (DSFM) (Vecchio 2000b) attempts to remove the main two issues of uncertainty of the above mentioned model, with the introduction of some corrections based on the results of experimental tests.

The model used in this paper to describe the behaviour of cracked concrete, under cyclic loads, is an improvement of existing procedures as based on a hybrid formulation between the model with full rotation of cracks and the model with fixed direction of cracking. The formulation described here, based on the theory of the modified compression field (MCFT), treats cracked concrete as a orthotropic material and involves a new approach for the evaluation of the re-orientation of both the compression field and the deformation field by removing the restriction of their coincidence.

2. Analysis of the reinforced concrete beam element

The model presented permits studying the behaviour of the generic section reinforced concrete beams subjected to cyclical stress. The theory is based on the following hypothesis:

1. hypothesis of preservation of plane sections by Bernoulli-Navier;
2. congruence of deformations;
3. the beam resists applied actions through a compression and diagonal traction field in the concrete, while the longitudinal and transversal reinforcement (stirrups), is subject to tensile or compression stresses;
4. the spacing of the stirrups is sufficiently limited to allow the creation of a space truss; each section along the beam can be considered identical to the others;
5. the deformations are small if compared to the dimensions of the section itself;
6. the torsion stress is uniform, and the secondary warping tensions are deemed negligible;
7. cyclical stresses are such as to exclude phenomena associated to material fatigue and the deterioration and/or collapse cannot be related to them;

8. cyclical stresses do not include those of an impulsive nature such as impacts and explosions. Stresses applied in restricted areas are not considered, in the shortest of times, such as to cause circumscribed damage to the region of application;
9. deformations due solely to shear are considered negligible.

The equivalent hollow section (Cocchi and Volpi 1996) is discretised into an n number of small elements with height B_i ($i = 1 \ldots n$) sufficiently small to formulate the hypothesis that the values of unknowns, tensions and deformations, are constant in each small element (Fig. 1). In order to avoid the double calculation of the portions of small angle elements which overlap in proximity of the vertices, the thickness t_d, the base B obtained for a rectangular small element are initially taken into

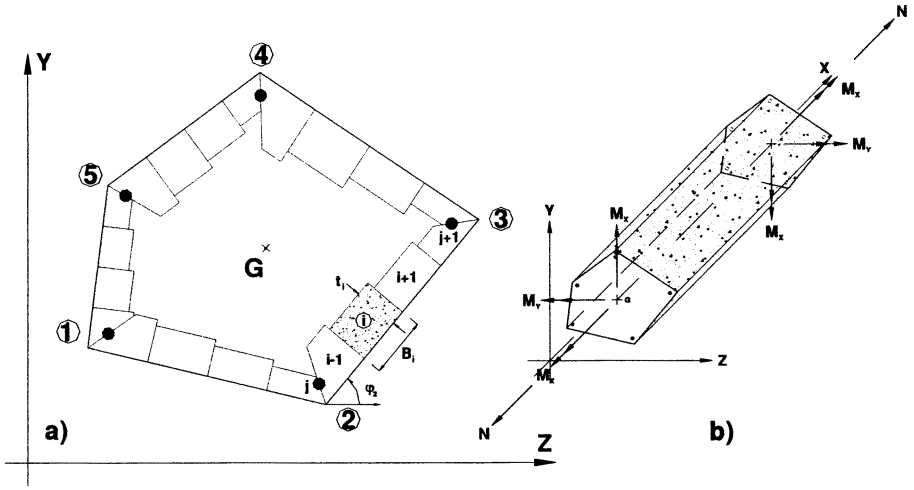

Fig. 1 Discretisation of a generic section in reinforced concrete

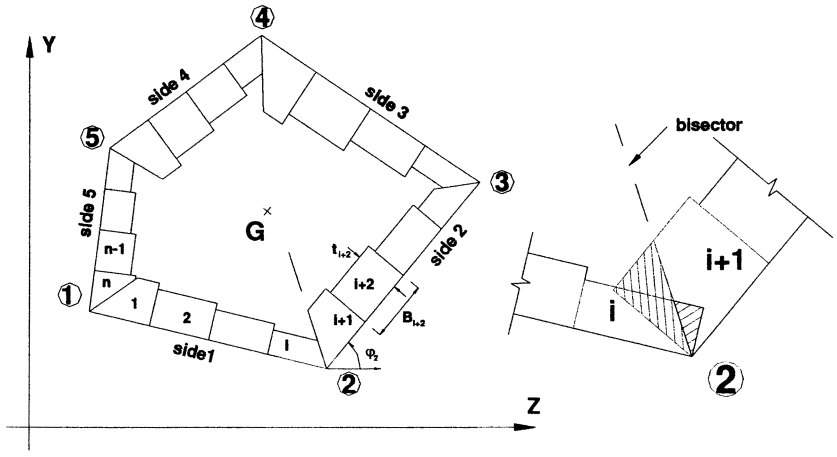

Fig. 2 Discretisation of the section subjected to torsion stress with adaptation of the small elements nearest to the vertex

consideration with subsequent adaptation deriving from the removal of the area of superimposition. In this way the angle small elements, initially rectangular in shape, are substituted by triangular or trapezoidal small elements and the side shared by two adjacent small elements is superimposed to the bisector of the internal angle of the section vertex (Fig. 2).

Discretisation causes discontinuity amongst the variables in proximity of the connections between the wall and angle small elements; by increasing the number of small elements the solution will converge to the exact solution.

With reference to the small element $\boldsymbol{x_i}$, according to hypothesis 1 it is possible to determine the longitudinal deformation ε_{li} calculated at the barycentre depending on the flexural curvatures χ_y, χ_z and longitudinal deformation η of the section.

$$\varepsilon_{l_i} = \eta - \chi_z \cdot y_{s_i} - \chi_y \cdot z_{s_i} \tag{1}$$

where

$$y_{s_i} = \frac{y_{P_i} + y_{P_{i+1}}}{2} + \frac{t_{d_i}}{2}\sin(\varphi_l + 90^o) \tag{2}$$

$$z_{s_i} = \frac{z_{P_i} + z_{P_{i+1}}}{2} + \frac{t_{d_i}}{2}\cos(\varphi_l + 90^o) \tag{3}$$

3. Relations of equilibrium

Consider the state of stress in a concrete element of the cracked beam: such an element, which is assumed to lie in the plane of the section is subjected to a set of stresses in the plane. Eq. (4) can also be proven using Mohr's circle.

$$\underline{\sigma} = \begin{pmatrix} \sigma_l \\ \sigma_t \\ \tau_{lt} \end{pmatrix} = \begin{pmatrix} \sigma_1\cos^2(\theta) + 2\tau_{12}\sin(\theta)\cos(\theta) + \sigma_2\sin^2(\theta) \\ \sigma_1\sin^2(\theta) - 2\tau_{12}\sin(\theta)\cos(\theta) + \sigma_2\cos^2(\theta) \\ 2\cdot[(\sigma_1 - \sigma_2)\sin(\theta)\cos(\theta) + \tau_{12}(\cos^2(\theta) - \sin^2(\theta))] \end{pmatrix} \tag{4}$$

According to the indications in (Vecchio 2000b) the equations of equilibrium of the element, are developed in terms of average and local tensions along the fracture surface.

The concrete is considered as an orthotropic material with a rotating direction of cracking in which the main average tensions f_{c1} and f_{c2} acting on the concrete are respectively perpendicular and parallel to the direction of cracking identified by the angle θ and the traction tension f_{c1} is still present after cracking because of the "*tension stiffening*" mechanism (Vecchio 2000b). The average tensions can also be considered as acting on the reinforcements. The tangential tensions v_{cr}, with respect to the interface of the crack, contribute to the equilibrium since they oppose the relative slippage of the edges of the crack itself.

Taking into account a unitary area in proximity of the two planes of direction 1 and 2, the equivalence of the external tensions applied (σ_x, σ_y, τ_{xy}) and the tensions on the planes 1 and 2 give the following relations:

$$[-\rho_{sl}(f_{slcr}-f_{sl}) + \rho_{st}(f_{stcr}-f_{st})]|\sin(\theta)\cos(\theta)| = -\nu_{cr} \tag{5}$$

$$\rho_{sl}(f_{slcr}-f_{sl})\cos^2(\theta) + \rho_{st}(f_{stcr}-f_{st})\sin^2(\theta) = -f_{c1} \tag{6}$$

$$\rho_{sl} = \frac{A_l}{B} \tag{7}$$

$$\rho_{st} = \frac{A_t}{\Delta x} \tag{8}$$

Note that (Vecchio and Collins 1986), in proximity of the crack, the tensile tension of the reinforcements is higher than that reached inside the concrete strut between one crack and another. Due to the adherence, the greater traction tension of the "bare" reinforcements is transferred to the concrete, thus reducing the traction tension of the steel.

The shear tension τ_{lt} due to torsion, intended as the average tension evenly spread over the thickness of the equivalent hollow section, gives rise to a flow of tangential tensions q which (Cocchi and Volpi 1996) are constant in the section according to translational equilibrium along the longitudinal axis of a portion of the beam between two straight sections.

The result for the case taken into account is:

$$q = \tau_{lt} \cdot t_d = \cos t \tag{9}$$

The global equilibrium of the equivalent hollow section, subjected to combined actions of torsion, axial force and biaxial flexure, is obtained by adding together the contributions of the internal tensions of all the small elements (Fig. 3)

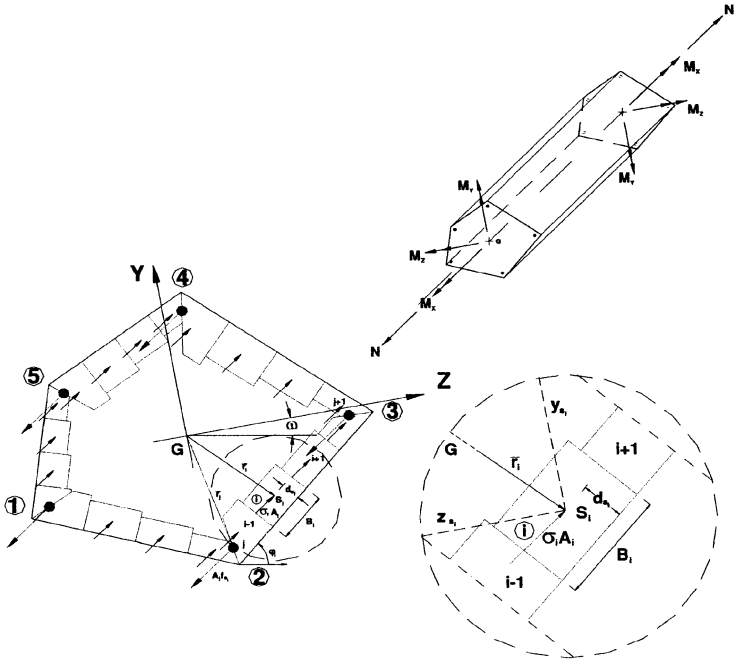

Fig. 3 Internal traction and compression tensions acting on the section capable of balancing external stresses

For axial force N we will have:

$$N = \sum_{i=1}^{n} \sigma_{l_i} A_i + \sum_{j=1}^{m} f_{sl_j}(\varepsilon_{l_j}) A_{s_j} \tag{10}$$

For bending moment M_y we will have:

$$M_y = -\sum_{i=1}^{n} \sigma_{l_i} A_i \cdot z_{s_i} - \sum_{j=1}^{m} f_{sl_j}(\varepsilon_{l_j}) A_{s_j} \cdot z_j \tag{11}$$

For bending moment M_z we will have:

$$M_z = -\sum_{i=1}^{n} \sigma_{l_i} A_i \cdot y_{s_i} - \sum_{j=1}^{m} f_{sl_j}(\varepsilon_{l_j}) A_{s_j} \cdot y_j \tag{12}$$

Each small element contributes to the balance of the twisting moment applied through the vector product between the resultant of the tangential tensions applied halfway up the thickness and the vector ray of its application point (point C_i), (Fig. 4) given by:

$$\underline{r}_i = z_{C_i}\underline{z} + y_{C_i}\underline{y} \tag{13}$$

The first can be expressed according to the coordinates of the vertices of the small element lying on the edge of the section, from the relation:

$$\hat{v}_i = \frac{(y_{P_{i+1}} - y_{P_i})}{\sqrt{(y_{P_{i+1}} - y_{P_i})^2 + (z_{P_{i+1}} - z_{P_i})^2}}\underline{y} + \frac{(z_{P_{i+1}} - z_{P_i})}{(y_{P_{i+1}} - y_{P_i})^2 + (z_{P_{i+1}} - z_{P_i})^2}\underline{z} \tag{14}$$

$$\overrightarrow{\tau_i A_i} = (\tau_i A_i)\hat{v}_i \tag{15}$$

For twisting moment M_x it is necessary:

$$M_x = \sum_{i=1}^{n} \underline{r}_i \wedge \overrightarrow{\tau_i A_i} \tag{16}$$

and the vector ray r_i, can be detected as soon as the position of the point of application (point C_i) of the resultant through Eqs. (2) and (3) is known.

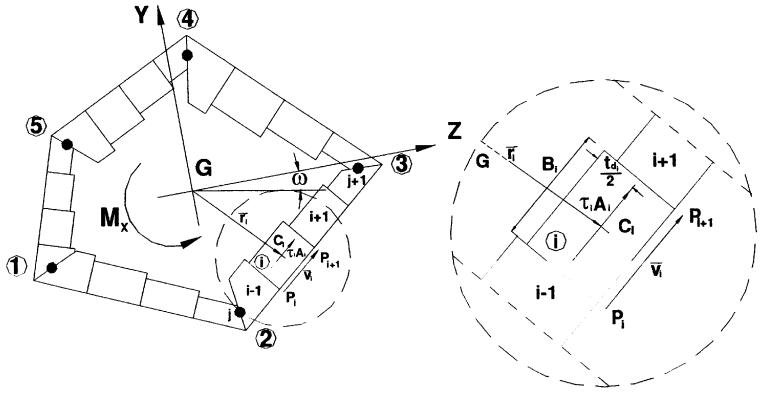

Fig. 4 Internal tangential tensions acting on the section capable of balancing external stresses

4. Relations of equilibrium

The deformations of a reinforced concrete beam are discontinuous and localised in restricted areas in which cracking makes the concrete non-homogeneous. The apparent or total deformation (Fig. 5c) are decomposed into two terms the first of which represents the deformation associated to the continuum (Fig. 5a) and the second expresses the deformation caused by the relative slippage along the cracks comparable to the deformation of a solid body (Fig. 5b)

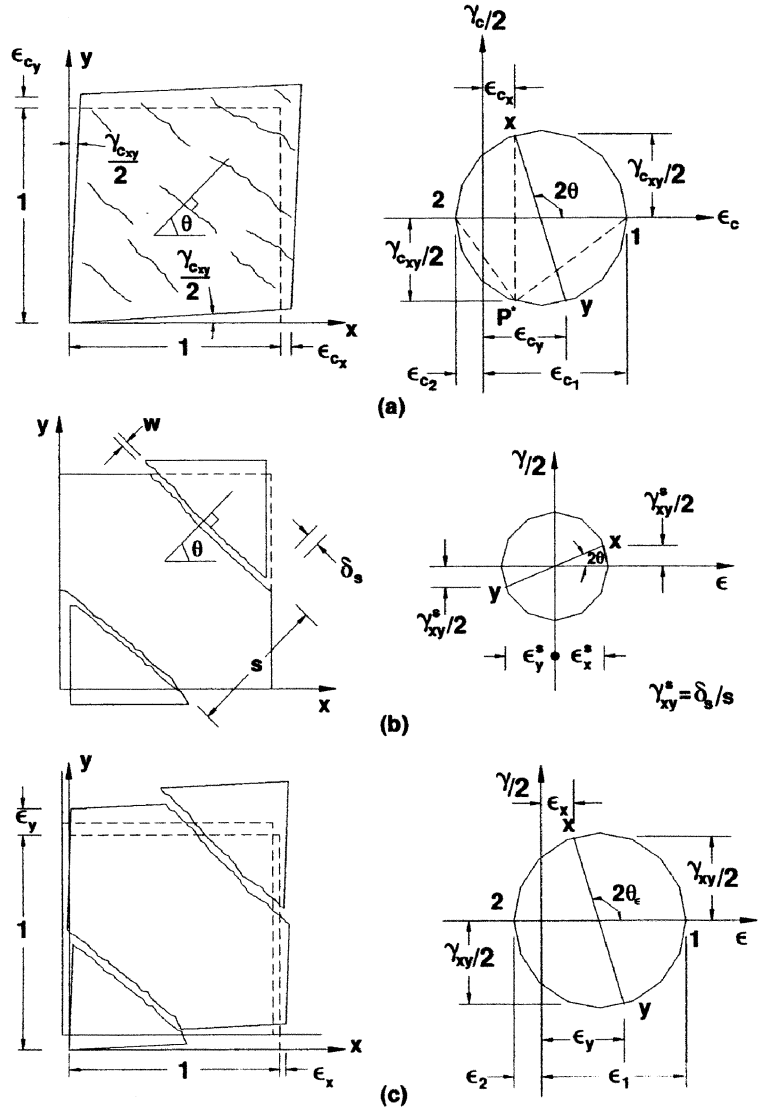

Fig. 5 Congruence relations: (a) deformations due to stresses in the continuum, (b) local deformations due to slippage along the fracture surfaces comparable *s* to the deformations of a solid body, (c) combination of the deformations

The vector of total deformations $\underline{\varepsilon}^T = (\varepsilon_x\ \varepsilon_y\ \gamma_{xy})$, makes it possible to pinpoint the direction of the main deformations through the well-known relation:

$$\theta_\varepsilon = \frac{1}{2} \cdot arc\tan\left(\frac{\gamma_{12}}{\varepsilon_1 - \varepsilon_2}\right) \tag{17}$$

in which θ_ε is different from the angle θ_σ of inclination of the main deformations in concrete considered as continuum, calculated by the relation:

$$\theta_\sigma = \frac{1}{2} \cdot arc\tan\left(\frac{\gamma_{c12}}{\varepsilon_{c1} - \varepsilon_{c2}}\right) \tag{18}$$

Considering that cracks begin to open when the tension in concrete is greater than the maximum traction tension, it can be supposed that the inclination of the cracks coincides with the direction of the main deformations in the concrete. According to this hypothesis the contribution of deformation having width w and interspace s connected to the slippage along the cracks, is:

$$\Delta\gamma_{12} = \frac{\delta_s}{s} \tag{19}$$

The space among the cracks is based on the suggested relation (Bhide and Collins 1989):

$$s = \frac{1}{\dfrac{\sin\theta}{s_{ml}} + \dfrac{\cos\theta}{s_{mt}}} \tag{20}$$

$$s_{ml} = 2 \cdot \left(c_l + \frac{s_l}{10}\right) + 0.1 \cdot \frac{d_{bl}}{\rho_l} \tag{21}$$

The total or apparent deformation is given by the sum of the single deformation contributions:

$$\underline{\varepsilon} = \begin{pmatrix} \varepsilon_1 \\ \varepsilon_2 \\ \gamma_{12} \end{pmatrix} = \underline{\varepsilon}^c + \underline{\varepsilon}^s + \underline{\varepsilon}^0 + \underline{\varepsilon}^p = \begin{pmatrix} \varepsilon_1^c \\ \varepsilon_2^c \\ \gamma_{12}^c \end{pmatrix} + \begin{pmatrix} \varepsilon_1^s \\ \varepsilon_2^s \\ \gamma_{12}^s \end{pmatrix} + \begin{pmatrix} \varepsilon_1^0 \\ \varepsilon_2^0 \\ \gamma_{12}^0 \end{pmatrix} + \begin{pmatrix} \varepsilon_1^p \\ \varepsilon_2^p \\ \gamma_{12}^p \end{pmatrix} \tag{22}$$

Deformations in direction 1 and 2 can be expressed according to those in direction *l-t* from the well-known relations (Pang and Hsu 1996):

$$\underline{\varepsilon} = \begin{pmatrix} \varepsilon_1 \\ \varepsilon_2 \\ \gamma_{12} \end{pmatrix} = \begin{pmatrix} \varepsilon_l\cos^2(\theta) + \gamma_{lt}\sin(\theta)\cos(\theta) + \varepsilon_t\sin^2(\theta) \\ \varepsilon_l\sin^2(\theta) - \gamma_{lt}\sin(\theta)\cos(\theta) + \varepsilon_t\cos^2(\theta) \\ 2 \cdot \left[(\varepsilon_l - \varepsilon_t)\sin(\theta)\cos(\theta) + \dfrac{\gamma_{lt}}{2}(\cos^2(\theta) - \sin^2(\theta))\right] \end{pmatrix} \tag{23}$$

Between the adjacent cracking surfaces, where the rod is practically “bare”, the reinforcement suffers an increase in deformation resulting in an increase of the tensions to compensate the local reduction of the traction tensions on the concrete, in order to guarantee equilibrium and inhibit the widening of the cracks, which can be estimated with the relation:

$$\Delta\varepsilon_1 = \frac{w}{s} \tag{24}$$

Given the hypothesis of perfect adherence between steel and concrete, the average deformation of the reinforcement can thus be calculated as follows:

$$\varepsilon_{sl} = \varepsilon_l + \varepsilon_{sl}^0 \tag{25}$$

$$\varepsilon_{st} = \varepsilon_t + \varepsilon_{st}^0 \tag{26}$$

while in proximity of the cracks the punctual deformation of the reinforcements is given by the sum of the average deformation and the increase in localised deformation. In the reference frame 1-2 the deformations in proximity of the cracks can be expressed as follows:

$$\underline{\varepsilon}_{cr}^{(1-2)} = \begin{pmatrix} \varepsilon_{1_{cr}} \\ \varepsilon_{2_{cr}} \\ \gamma_{12_{cr}} \end{pmatrix} = \begin{pmatrix} \varepsilon_1 + \Delta\varepsilon_1 \\ \varepsilon_2 \\ \gamma_{12} + \Delta\gamma_{12} \end{pmatrix} = \begin{pmatrix} \varepsilon_{l_{cr}}\cos^2(\theta) + \gamma_{lt_{cr}}\sin(\theta)\cos(\theta) + \varepsilon_{t_{cr}}\sin^2(\theta) \\ \varepsilon_{l_{cr}}\sin^2(\theta) - \gamma_{lt_{cr}}\sin(\theta)\cos(\theta) + \varepsilon_{t_{cr}}\cos^2(\theta) \\ 2\cdot\left[(\varepsilon_{l_{cr}} - \varepsilon_{t_{cr}})\sin(\theta)\cos(\theta) - \frac{\gamma_{lt_{cr}}}{2}(\cos^2(\theta) - \sin^2(\theta))\right] \end{pmatrix} \tag{27}$$

Considering that $\gamma_{12} = 0$ in that the reference frame 1-2 is a principal reference frame, we have:

$$\underline{\varepsilon}_{cr}^{(l-t)} = \begin{pmatrix} \varepsilon_{l_{cr}} \\ \varepsilon_{t_{cr}} \\ \gamma_{lt_{cr}} \end{pmatrix} = \begin{pmatrix} (\varepsilon_1 + \Delta\varepsilon_1)\cos^2(\theta) + \Delta\gamma_{12}\sin(\theta)\cos(\theta) + \varepsilon_2\sin^2(\theta) \\ (\varepsilon_1 + \Delta\varepsilon_1)\sin^2(\theta) - \Delta\gamma_{12}\sin(\theta)\cos(\theta) + \varepsilon_2\cos^2(\theta) \\ 2\cdot\left[((\varepsilon_1 + \Delta\varepsilon_1) - \varepsilon_2)\sin(\theta)\cos(\theta) - \frac{\Delta\gamma_{12}}{2}(\cos^2(\theta) - \sin^2(\theta))\right] \end{pmatrix} \tag{28}$$

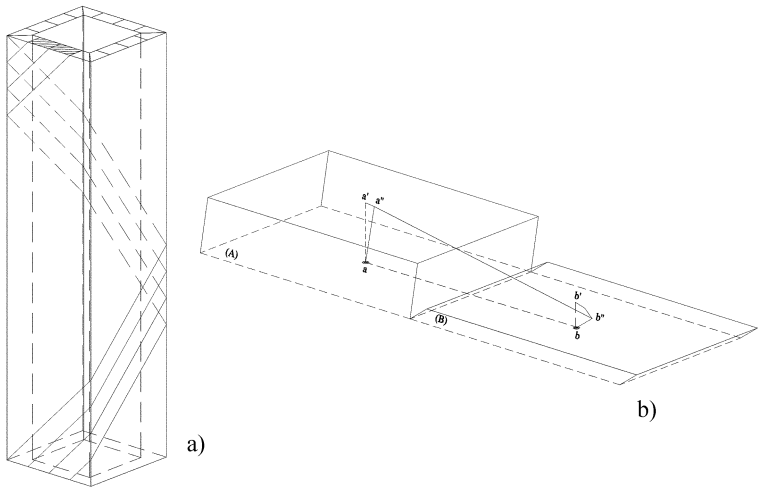

Fig. 6 Discretisation of the section and deformation (a) helical fracture curvatures, (b) deformation of two adjacent small elements

As far as congruence between the deformations of the small elements is concerned, it can be noted that the hypothesis due to the classic treatment by Vlasov (1961) involves unrealistically high rigidities, contrary to experimental evidence, especially in the nonlinear and ultimate fields.

As shown by Fig. 6, the deformation of the medium line ε_t can be estimated as follows.

Two adjacent small elements A and B with a and b as the respective points of application of the resultants of the tangential tensions (Fig. 6b), are considered.

When the small element A (respectively B) suffers a longitudinal deformation ε_l equal to aa' (respectively bb') and a tangential deformation γ_{lt} equal to $a'a''$ (respectively $b'b''$) once the deformation has occurred, the distance ab will be equal to $a''b''$. The deformation of the medium line ε_t is:

$$\varepsilon_t = \frac{\overline{a''b''} - \overline{ab}}{\overline{ab}} = \frac{\overline{a''b''}}{\overline{ab}} - 1 \tag{29}$$

from which we obtain:

$$\varepsilon_t = \frac{\sqrt{(\overline{ab} + \gamma_{lt}^{(A)} - \gamma_{lt}^{(B)})^2 + (\varepsilon_l^{(A)} - \varepsilon_l^{(B)})^2}}{\overline{ab}} - 1 \tag{30}$$

by expressing the axial and tangential deformations of each small element.

Eq. (30) expresses the congruence of each small deformed element with respect to that adjacent to the same.

A further equation of congruence can be obtained from the principle of virtual works by imposing equality between the external work, due to the applied axial, flexural and twisting actions and the internal work due to inner stresses:

$$L_e(\eta, \chi_x, \chi_y, \chi_z, N, M_x, M_y, M_z) = L_i(\varepsilon_x, \varepsilon_y, \gamma_{xy}, \sigma_x, \sigma_x, \tau_{xy}) \tag{31}$$

In the proposed treatment, the principle of virtual works makes it possible to single out the only congruent configuration amongst the equilibrated infinites.

Note that in Eq. (31) a hypothesis is formulated whereby the energy subtracted from the system and dispersed in heat and energy to degrade the edges of the cracks, is of an almost negligible quantity with respect to the terms contained in the same.

By expressing the external work according to the applied stresses and the "macroscopic" deformations involving the entire beam, and the internal work according to the tensions and internal deformations, we have:

$$N\eta + M_x\chi_x + M_y\chi_y + M_z\chi_z = \sum_{i=1}^{n} \sigma_{l_i} A_i \varepsilon_{l_i} + \sum_{i=1}^{n} \tau_{lt_i} A_i \gamma_{lt_i} + \sum_{j=1}^{n} f_{sl_j} A_{s_j} \varepsilon_{l_j} \tag{32}$$

5. Constitutive laws

5.1 Concrete

The following (Vecchio 2000b) is used for compressed concrete under a condition of biaxial stress:

$$f_{c2(base)} = -f_p \cdot \frac{n \cdot \frac{-\varepsilon_{c2}}{\varepsilon_p}}{n - 1 + \left(\frac{-\varepsilon_{c2}}{\varepsilon_p}\right)^{n \cdot k}} \tag{33}$$

with

$$n = 0.80 \cdot \frac{f_p}{17} \tag{34}$$

$$k = \begin{cases} 0.67 - \frac{f_p}{62} & \text{if} \quad \varepsilon_p > \varepsilon_{c2} \\ 1.0 & \text{if} \quad \varepsilon_p < \varepsilon_{c2} < 0 \end{cases} \tag{35}$$

A softening factor β_d is used to define both peak strength f_p and peak deformation ε_p of the concrete subjected to compression as for the following equation (Vecchio 2000b):

$$f_p = -\beta_d \cdot f_c' \tag{36}$$

$$\varepsilon_p = -\beta_d \cdot \varepsilon_0 \tag{37}$$

The softening coefficient assumes the following value:

$$\beta_d = \frac{1}{1 + C_s \cdot C_d} \leq 1.0 \tag{38}$$

The C_d factor is a function of the relation $\varepsilon_{c1}/\varepsilon_{c2}$ and precisely:

$$C_d = 0.35\left(-\frac{\varepsilon_{c1}}{\varepsilon_{c2}} - 0.28\right)^{0.8} \tag{39}$$

and the factor C_s assumes the following value:

$$C_S = 0.55 \tag{40}$$

Resistance to compression of concrete is influenced by the width of the cracks as follows:

$$f_{c2} = \begin{cases} f_{c2}' & \text{if} \quad w < 2 \\ f_{c2}' \cdot \frac{5 - w}{3} & \text{if} \quad 2 \leq w \leq 5 \\ 0 & \text{if} \quad w > 5 \end{cases} \tag{41}$$

In the case of concrete subjected to traction, before cracking, a linear relation of the following kind is used:

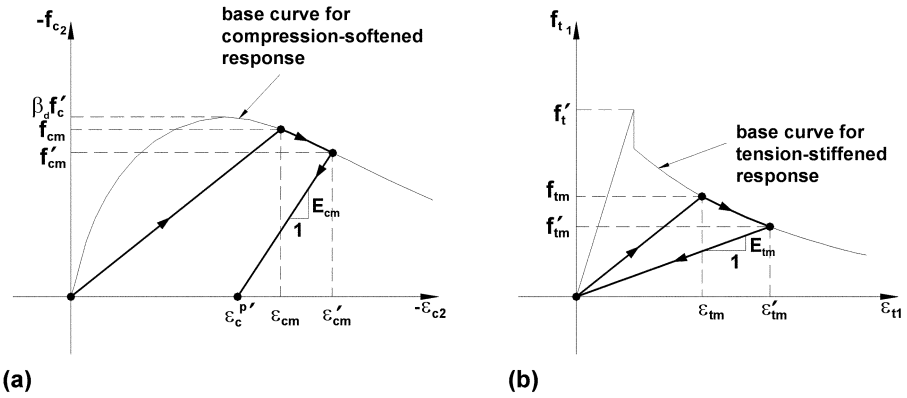

Fig. 7 Hysteretical model for concrete: (a) response to compression, (b) response to traction

$$f_{c1} = E_c \cdot \varepsilon_{c1} \quad \text{if} \quad 0 < \varepsilon < \varepsilon_{cr} \tag{42}$$

The contribution of "*tension stiffening*" can be estimated according to the following relation:

$$f_t = 0.65 \cdot (f_c')^{0.33} \tag{43}$$

The "*tension stiffening*" coefficient can be expressed through the relation suggested by Bentz (Vecchio 2000b):

$$f_{c1}^{(stiff.)} = \frac{f_t}{1 + \sqrt{c_t \cdot \varepsilon_{c1}}} \tag{44}$$

In order to describe the response of concrete subjected to cyclical stresses, a group of equations, connected to the curve envelope described previously (Vecchio 2000b), is used. These describes monotonous behaviour, and require knowledge of all the pre-existing maximum deformations. In a continuum, where the principal directions of deformation vary from point to point in the concrete, the problem can be faced thanks to the proposed method, based on the application of Mohr's circle.

The constitutive laws for cyclical stresses, adopted during the proposed procedure, are based on essentially linear rules of unloading/reloading

The compression constitutive law is illustrated in Fig. 7(a) for each of the principal directions of deformation (i.e., $\varepsilon_c = \varepsilon_{c1}$ o $\varepsilon_c = \varepsilon_{c2}$; the other parameters are consequentially deductible).

In a reloading cycle, where residual plastic deformation of concrete is $\varepsilon_c^{p'}$, the compression stress is calculated as follows:

$$f_c(\varepsilon_c) = \begin{cases} 0 & \text{if} \quad \varepsilon_c > \varepsilon_c^p \quad \text{or} \quad \varepsilon_c > 0 \\ (\varepsilon_c - \varepsilon_c^p) \cdot \dfrac{f_{cm}}{\varepsilon_{cm} - \varepsilon_c^p} & \text{if} \quad \varepsilon_c^p > \varepsilon_c - \varepsilon_{cm} \\ f_{bc}(\varepsilon_c) & \text{if} \quad \varepsilon_c < \varepsilon_{cm} \end{cases} \tag{45}$$

Deformations ε_c and ε_{cm} are total deformations and include plastic deformation. If tension falls on the curve envelope (i.e., $\varepsilon_c < \varepsilon_{cm}$) then ε_{cm} and f_{cm} are respectively updated to ε'_{cm} and f'_{cm}. At each loading stage, instant plastic deformation $\varepsilon_c^{p\prime}$ is given by the following expression (Vecchio 1999):

$$\varepsilon_c^{p\prime} = \begin{cases} \varepsilon_c - \varepsilon_p\left[0.87 \cdot \left(\frac{\varepsilon_c}{\varepsilon_p}\right) - 0.29 \cdot \left(\frac{\varepsilon_c}{\varepsilon_p}\right)^2\right] & \text{if} \quad \varepsilon_c > 1.5 \cdot \varepsilon_p \\ \varepsilon_c - 0.001305 \cdot \left(\frac{\varepsilon_c}{0.002}\right) & \text{if} \quad \varepsilon_c < 1.5 \cdot \varepsilon_p \end{cases} \tag{46}$$

If instant plastic deformation $\varepsilon_c^{p\prime}$ exceeds plastic deformation ε_c^p, then the latter is consequently updated.

During unloading, phase tensions are generated which can be estimated according to the following expression:

$$f_c(\varepsilon_c) = E_{cm} \cdot (\varepsilon_c - \varepsilon_c^p) \tag{47}$$

$$E_{cm} = \frac{f_{cm}}{(\varepsilon_{cm} - \varepsilon_c^{p\prime})} \tag{48}$$

This model implies the simplified hypothesis whereby during a recurrent excursion from the domain of traction deformations, compression stresses are null until the cracks close themselves completely (i.e., until $\varepsilon_c < 0$).

The constitutive traction law, illustrated in Fig. 7(b), uses a base curve consisting of two parts: one which describes the pre-cracking defined by Eq. (42) and one which represents the post-cracking response due to "*tension stiffening*" defined by Eq. (44).

In a reloading cycle, traction tension in concrete is calculated as follows:

$$f_t(\varepsilon_t) = \begin{cases} \frac{(\varepsilon_t - \varepsilon_t^p)}{(\varepsilon_{tm} - \varepsilon_t^p)} \cdot f_{tm} & \text{if} \quad \varepsilon_t^p \le \varepsilon_t \le \varepsilon_{tm} \\ f_{bt}(\varepsilon_t) & \text{if} \quad \varepsilon_t \ge \varepsilon_{tm} \end{cases} \tag{49}$$

$$\varepsilon_t^{p\prime} = \begin{cases} \varepsilon_t & \text{if} \quad \varepsilon_t^p < \varepsilon_t < 0 \\ 0 & \text{if} \quad \varepsilon_t \ge 0 \end{cases} \tag{50}$$

In proximity of the first traction cycle, plastic deformation ε_t^p, is kept constant at the determined value when the tension relates to the compression domain. The deformation used for the calculation along the base curve, is free of plastic deformation so that the base curve is translated in such a way that its origin coincides with ε_t^p. In successive cycles plastic deformation is redefined as follows: when the response falls on the curve envelope ($\varepsilon_t < \varepsilon_{tm}$), maximum traction deformation and the corresponding tension are respectively updated to ε'_{tm} and f_{tm} (Fig. 7b). Tension during unloading can be calculated as follows:

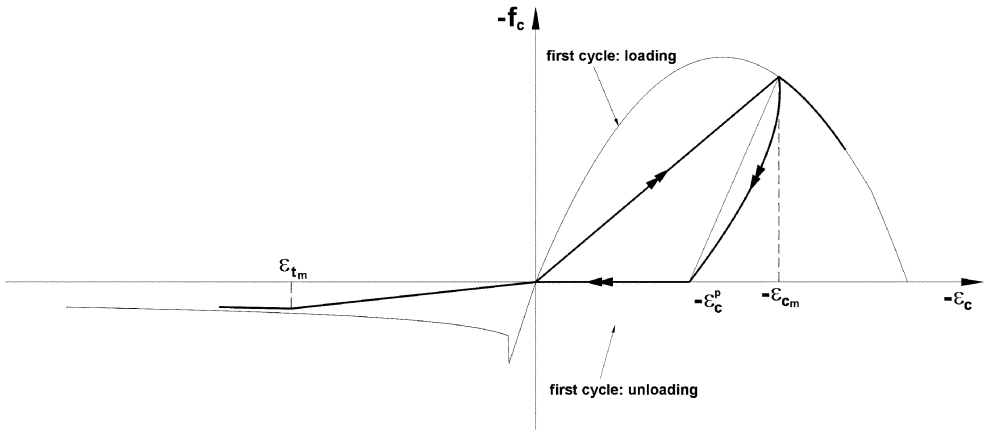

Fig. 8 Constitutive law for cyclically stressed concrete

$$f_t(\varepsilon_t) = E_{tm} \cdot (\varepsilon_t - \varepsilon_t^p) \tag{51}$$

where the tensile module during unloading is defined as:

$$E_{tm} = \frac{f'_{tm}}{(\varepsilon'_{tm} - \varepsilon_c^p)} \tag{52}$$

In conclusion the constitutive law for concrete subjected to cyclical stresses used by this treatment is shown in Fig. 8.

5.2 Steel

The constitutive law for steel used (Elmosieri *et al.* 1998) (Fig. 9) is described by a curve composed of two straight lines (Prantdl's bilateral). The first line has a slope equal to E_0 and the second has a slope equal to E_1, both generating asymptotes for the constitutive law:

$$\sigma_s^* = b \cdot \varepsilon^* + \frac{(1-b) \cdot \varepsilon^*}{(1 - \varepsilon^{*R})^{1/R}} \tag{53}$$

$$\sigma^* = \frac{(\sigma - \sigma_r)}{(\sigma_0 - \sigma_r)} \tag{54}$$

$$\varepsilon^* = \frac{(\varepsilon - \varepsilon_r)}{(\varepsilon_0 - \varepsilon_r)} \tag{55}$$

$$R = R_0 + \frac{a_1 \cdot \xi}{a_2 + \xi} \tag{56}$$

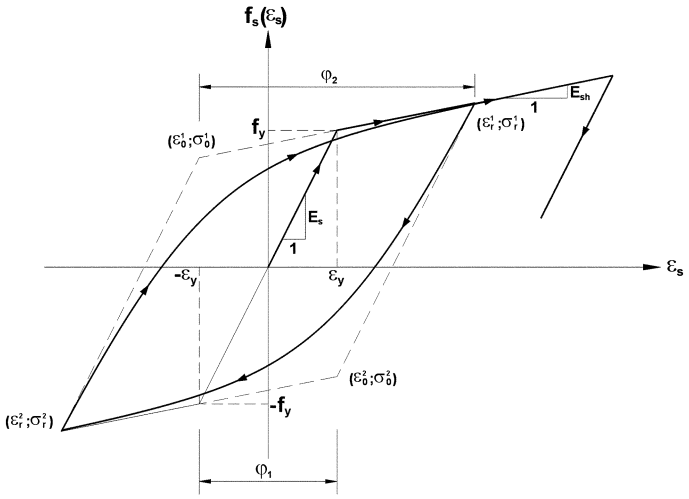

Fig. 9 Constitutive law for steel by Pinto and Menegotto (1977) for cyclical loading

Note that even in this case, in order to fully describe the behaviour of steel subjected to cyclical stresses, in addition to knowing the mechanical characteristics required for the construction of the base curve, it is also necessary to know the history of deformations occurring during the last loading/unloading stage.

5.3 Considerations on the shear tensions at the interface of the cracks

In the past twenty years methods have been developed for the calculation of tangential tensions that occur at the cracks interface due to friction.

When shear tension is applied to a cracked element, slippage occurs between the edges of the cracks accompanied by the inevitable detachment of the same edges caused by the roughness of the fracture surface (Ali and White 1999).

The detachment of the crack edge causes an increase of the traction tensions in the reinforcements which, due to the steel/concrete adherence, transform into compression forces acting on the interface, capable of preventing further opening of the cracks.

In conclusion, many factors influence the calculation of the tangential tensions and each is itself a function of a series of variables of a stochastic nature such as shape and nature of the aggregate, resistance of the concrete, lack of internal resistance and any other component in the "*mix design*" of the concrete conglomerate; for this reason, the determination of a reliable model requires a statistical approach based on the regression of the data obtained through a series of tests carried out on samples, with an elaboration of numerical formulations that is difficult to apply.

According to the data obtained by the experimental tests started by Paulay and Loeber, Bazant and Gambarova (1987) the following relation is suggested to determine the ultimate shear resistance of concrete:

$$v_{cr} = \tau_{\max} r \cdot \frac{a_3 + a_4 |r|^3}{1 + a_4 r^4} \tag{57}$$

$$\tau_{\max} = 0.245 \cdot f_c' \frac{c^2}{c^2 + 100 \cdot w^2} \tag{58}$$

$$\sigma = -\frac{0.534}{1000 \cdot w} (145 |v_{cr}|)^p \tag{59}$$

$$r = \frac{\delta_s}{w} \tag{60}$$

$$a_3 = \frac{10}{f_c'} \tag{61}$$

$$a_4 = 2.44 - \frac{39.8}{f_c'} \tag{62}$$

In the case of repeated loading cycles, which are the subject matter of this paper, it should be noted that the importance of tangential tensions v_{cr}, decreases as the cycles increase following the reduction of the degree of roughness on the fracture surfaces in the presence of the crashing and expulsion of aggregates in the cement matrix of the concrete.

6. Algorithm for the solution of the nonlinear equations system

Once the constitutive laws for concrete, for longitudinal steel and for the stirrups have been assigned, together with the geometrical characteristics of the sections and the stresses applied, it is necessary to determine the number of unknowns strictly required to fully describe the deformation and tensional states of the beam element.

For each small element, subdividing the section, the five unknowns ε_{li}, ε_{ti}, γ_{lti}, w_i, δ_{si} are taken as independent variables. For each section the unknowns η, χ_x, χ_y, χ_z, q, are considered. It is necessary to determine a total of $5 \cdot n + 5$ independent unknown variables.

The equations obtained in the previous paragraphs which determine the problem for each small element are:

Eqs. (5) and (6) of local equilibrium, Eq. (30) of transversal deformation congruence, Eq. (1) of preservation of the plane sections and Eq. (9) of the translational equilibrium in longitudinal direction for the generic section;

Eq. (32) of the principle of virtual works, Eq. (10) of the translational equilibrium in longitudinal direction, Eq. (16) of equilibrium to the rotation around the longitudinal axis x (torsion), Eq. (11) of equilibrium to the rotation around the axis y (flexure) and Eq. (12) of equilibrium to the rotation around the axis z (flexure).

A total of $5 \cdot n + 5$ nonlinear independent equations are available. The nonlinear simultaneous equations, in homogenous form, can be thus rewritten:

$$
\begin{cases}
F_{1_i} = [-\rho_{sl_i}(f_{slcr_i} - f_{sl_i}) + \rho_{st_i}(f_{stcr_i} - f_{st_i})] \cdot |\sin(\theta_i)\cos(\theta_i)| + \nu_{cr_i} = 0 \\
F_{2_i} = \rho_{sl_i}(f_{slcr_i} - f_{sl_i})\cos^2(\theta_i) + \rho_{st_i}(f_{stcr_i} - f_{st_i})\sin^2(\theta_i) - f_{c1_i} = 0 \\
F_{3_i} = \varepsilon_t - \dfrac{\sqrt{(\overline{a_i a}_{i+1} + \gamma_{lt_i} - \gamma_{lt_{i+1}})^2 + (\varepsilon_{l_i} - \varepsilon_{l_{i+1}})^2}}{\overline{a_i a}_{i+1}} + 1 = 0 \\
F_{4_i} = \varepsilon_{l_i} - \eta - \chi_z \cdot y_{c_i} + \chi_y \cdot z_{c_i} = 0 \\
F_{5_i} = \tau_{lt_1} \cdot t_{d_i} - q = 0 \\
\ldots\ldots\ldots\ldots\ldots\ldots\ldots\ldots\ldots\ldots\ldots\ldots\ldots\ldots \\
\ldots\ldots\ldots\ldots\ldots\ldots\ldots\ldots\ldots\ldots\ldots\ldots\ldots\ldots \\
F_1 = \sum_{i=1}^{n} \sigma_{l_i} A_i \varepsilon_{l_i} + \sum_{i=1}^{n} \tau_{lt_i} A_i \gamma_{lt_i} + \sum_{j=1}^{n} f_{sl_j} A_{s_j} \varepsilon_{l_j} - N\eta - M_x\chi_x - M_y\chi_y - M_z\chi_z = 0 \\
F_2 = \sum_{i=1}^{n} \sigma_{l_i} A_i + \sum_{j=1}^{m} f_{sl_j} A_{s_j} - N = 0 \\
F_3 = \sum_{i=1}^{n} \vec{r}_i \wedge \overrightarrow{\tau_i A_i} - M_x = 0 \\
F_4 = \sum_{i=1}^{n} \sigma_{l_i} A_i \cdot z_{s_i} + \sum_{j=1}^{m} f_{sl_j} A_{s_j} \cdot z_j + M_y = 0 \\
F_5 = \sum_{i=1}^{n} \sigma_{l_i} A_i \cdot y_{s_i} + \sum_{j=1}^{m} f_{sl_j} A_{s_j} \cdot y_j + M_z = 0
\end{cases}
\tag{63}
$$

where

i = 1, 2, …n;

j = 1, 2, …m;

Note that the equations, involving a small generic element, are functions solely of the unknowns concerning it (ε_l, ε_t, γ_{lt}, w, δ_s) and of the global unknowns common to all the elements (η, χ_x, χ_y, χ_z, q) while the global equations involve all the unknowns of the problem. For these reasons the resolving equations are coupled.

A Taylor expansion of the first order can be used to make system (63) linear:

$$
\underline{\underline{J}}(\underline{x}_0)(\underline{x} - \underline{x}_0) = -\underline{f}(\underline{x}_0) \tag{64}
$$

where

$\underline{\underline{J}}(\underline{x}_0)$ is the Jacobian matrix:

$$\underline{\underline{J}}(\underline{x}_0) = \begin{bmatrix} \dfrac{\partial f_1(x_{0_1}, x_{0_2}, \ldots, x_{0_n})}{\partial x_1} & \dfrac{\partial f_1(x_{0_1}, x_{0_2}, \ldots, x_{0_n})}{\partial x_2} & \cdots & \dfrac{\partial f_1(x_{0_1}, x_{0_2}, \ldots, x_{0_n})}{\partial x_n} \\ \dfrac{\partial f_2(x_{0_i}, x_{0_2}, \ldots, x_{0_n})}{\partial x_1} & \dfrac{\partial f_2(x_{0_1}, x_{0_2}, \ldots, x_{0_n})}{\partial x_2} & \cdots & \dfrac{\partial f_2(x_{0_1}, x_{0_2}, \ldots, x_{0_n})}{\partial x_n} \\ \cdots & \cdots & \cdots & \cdots \\ \dfrac{\partial f_n(x_{0_1}, x_{0_2}, \ldots, x_{0_n})}{\partial x_1} & \dfrac{\partial f_n(x_{0_1}, x_{0_2}, \ldots, x_{0_n})}{\partial x_2} & \cdots & \dfrac{\partial f_n(x_{0_1}, x_{0_2}, \ldots, x_{0_n})}{\partial x_n} \end{bmatrix}$$

$\underline{f}(\underline{x}_0)$ is the vector of known terms:

$$\underline{f}(\underline{x}_0) = \begin{pmatrix} f_1(x_{0_1}, x_{0_2}, \ldots, x_{0_n}) \\ f_2(x_{0_1}, x_{0_2}, \ldots, x_{0_n}) \\ \ldots\ldots\ldots\ldots\ldots\ldots \\ f_n(x_{0_1}, x_{0_2}, \ldots, x_{0_n}) \end{pmatrix}$$

$(\underline{x} - \underline{x}_0)$ is the solution vector:

$$(\underline{x} - \underline{x}_0) = \begin{pmatrix} x_1 - x_{0_1} \\ x_2 - x_{0_2} \\ \ldots\ldots\ldots \\ x_n - x_{0_n} \end{pmatrix}$$

The solution of the system (63), as it is known, can be obtained by Newton-Raphson's iterative method, for the $i + 1$ iteration:

$$\underline{x}_{i+1} = \underline{x}_i - \underline{\underline{J}}^{-1}(\underline{x}_i)\, \underline{f}(\underline{x}_i) \tag{65}$$

In order to solve the problem of the derivation of the implicit system functions (63) interpolation through polynomials is applied:

$$f(x) \cong p(x) = \sum_{k=0}^{g} a_k x^k \tag{66}$$

$$f'(x) \cong p'(x) = \sum_{k=1}^{g} k a_k x^{k-1} \tag{67}$$

In order to solve the linear system (65), the Gauss pivotal method is applied. This choice was made because the Jacobian matrix (64) is sparse non symmetrical with non prevailing terms on the principal diagonal.

7. Calculation procedure

The proposed method has been implemented in a procedure for computational calculation consisting of the following main steps (Fig. 10):

1. after assigning the physical-geometrical characteristics of the beam and the stresses, the section is divided in a predetermined sufficiently high number of small elements;
2. the intensity of cyclical stress is calculated by varying the temporal parameter characterising the modulated cosine (Fig. 11)

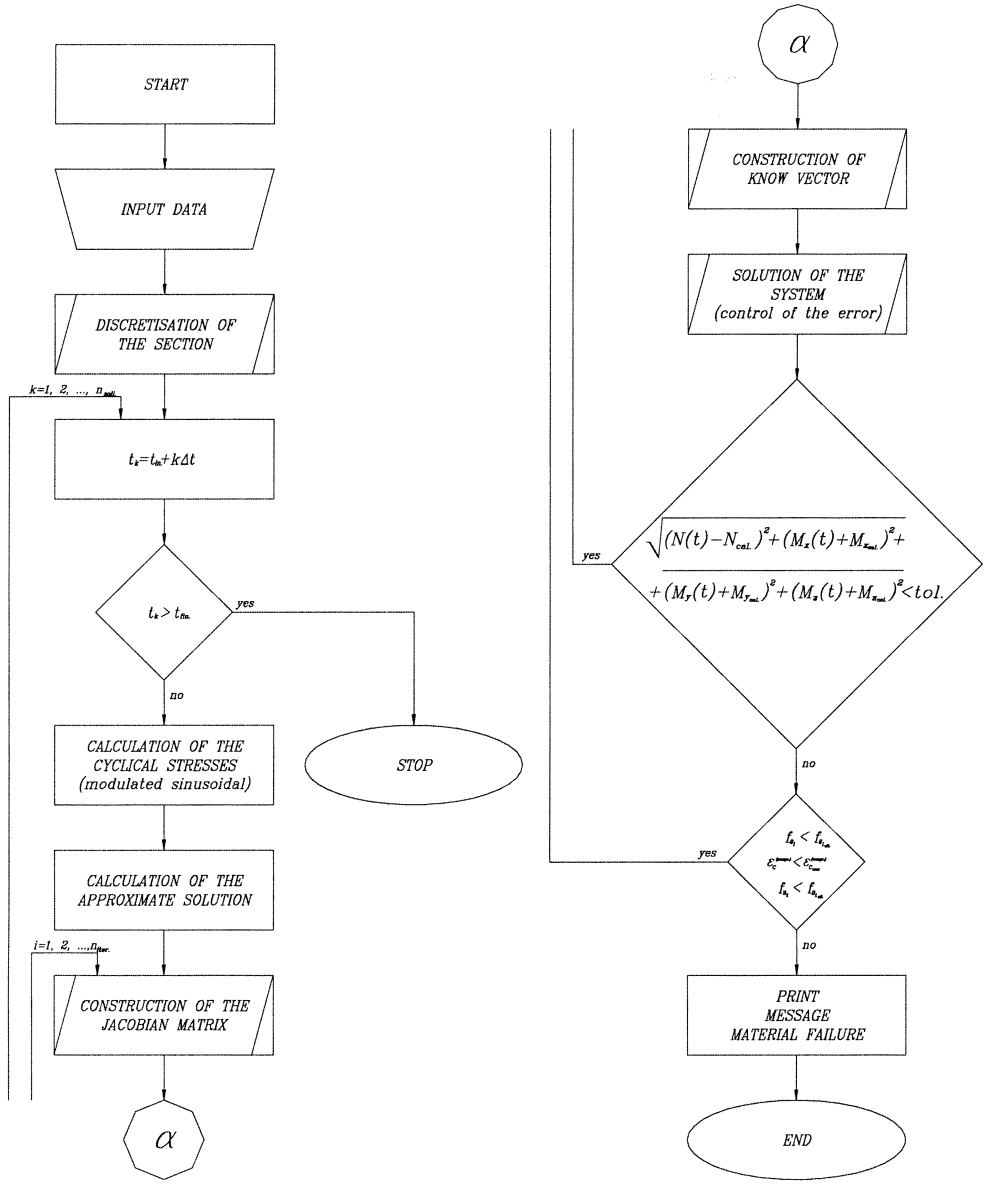

Fig. 10 Flow-chart of proposed procedure

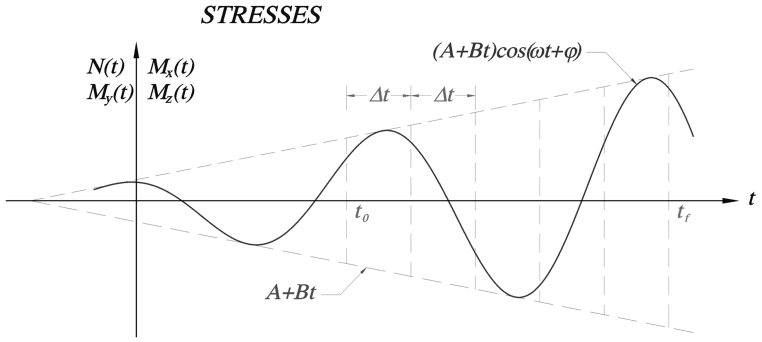

Fig. 11 Stresses of a modulated sinusoidal

3. an initial approximate start point is determined for the Newton-Raphson formula (65), calculated according to the De Saint Venant theory, depending on the stresses applied;
4. the Jacobian matrix is assembled with the calculation of the gradient vector of each function of (63) through the method of differentiation of the approximated polynomials;
5. the vector of known terms is assembled by calculating the values assumed by each function of (63) at the initial solution step;
6. the solution is calculated with the Newton-Raphson method in the matrix form described in Eq. (65) by the pivotal Gauss elimination and subsequent reverse substitution with error control until the desired accuracy is attained;
7. global stresses are calculated and compared with those assigned; if the differences in the solutions obtained in steps i, $i + 1$ exceed a predetermined tolerance value, the procedure restarts from step 4.

8. Results of the nonlinear analysis of beam elements subject to cyclical stresses

The analysis of the following beam elements is important to verify the utility of the calculation procedure proposed in order to study complex behaviours and the interactions of complex structures. Even so, the most important item in the study of the fundamental constitutive behaviour of cyclically stressed reinforced concrete is that obtained thanks to simple elements subjected to well defined and well controlled loads.

Figs. 12-24 show the numerical results obtained with the procedure proposed for some reinforced concrete beam elements with hollow rectangular sections (Figs. 12, 15), hollow octagonal sections (Figs. 17 and 20) and solid rectangular sections (Figs. 21 and 24) subjected to cyclical stresses deriving from torsion, axial stress and sinusoidal flexure, modulated as indicated in Fig. 11, considering that the equation described below makes it possible to simulate the loading conditions which generally occur in the engineering field.

Such elements have already been object of experimental (Hsu and Mo 1985) and numerical (Cocchi and Volpi 1996) investigation in the case of static stresses.

According to author's knowledge experimental results relevant to beam elements subjected to cyclical combined actions of torsion, biaxial flexure and axial forces are not currently available. Nevertheless direct comparison with the numerical and experimental results, in the static case, show

that the proposed MCFT/DSFM formulation describe realistically the non-linear behaviour of the beam elements tested.

In order to reach a sufficient degree of accuracy in reasonable calculation times, the sections analysed have been subdivided into sixteen small elements, since it was noted that an excessive subdivision increases the accuracy of the solution negligibly while it significantly increases the calculation time. It was observed in fact that the discrepancy between the solution obtained by subdividing the section into twenty small elements and that obtained by subdividing it into twenty-four small elements is far too negligible to justify the significant increase in the calculation time. Cyclical stresses were imposed by specifying the value of the temporal variable t representing the argument of the modulated sinusoid (Fig. 11) which was increased at every cycle through to collapse. Starting from an approximate solution obtained with the application of the technical theory of the beam, the calculation algorithm searched for the solution of the problem by successive approximations improving the previous solution until the difference between applied and calculated stresses is less than a pre-established tolerance fixed, for this analysis, at 250

$$\sqrt{(N(t)-N_{cal.})^2+(M_x(t)-M_{x_{cal.}})^2+(M_y(t)-M_{y_{cal.}})^2+(M_z(t)-M_{z_{cal.}})^2}\leq tolerance \qquad (68)$$

If the deformations of materials - steel and concrete - do not exceed their own ultimate deformations, the temporal variable t is increased and the calculation is repeated until one of the materials breaks. This analysis confirmed that the algorithm proposed is extremely stable and that it converges at every loading phase.

Observing the action-deformation diagrams obtained through the numerical analysis and shown in the pictures below, a prevailing tendency to fragility is detected in the elements tested.

The progressive addition of a further external action such as axial stress and/or bending moment, reduces the importance of homologous deformations with a drastic decrease in the number of the cycles required to bring the beam element to breaking point. The beam elements analysed reach collapse after exceeding the breaking tension in the stirrups since significant deformation tend to concentrate in the fracture areas where the reinforcement is “bare” and thus more sensitive to deformation.

A discrepancy is noted between the experimental (Walvaren 1981) and the theoretical values of v_{cr} as a function of the relative slippage δ, obtained through the formulations suggested by various authors: each function is closer to the experimental values only at a certain interval.

Furthermore, some of the formulations illustrated rise, meaning that, as the width of the cracks w_i and the relative slippage δ -grow, tangential tension reaches unacceptable values.

Furthermore it was observed that the effect of the tangential tensions at the interface of the cracks significantly influences the tensional-deformation state of the tested beam element. In order to substantiate the importance of this factor, the numerical analysis was repeated and Eq. (57) was substituted with the those with an increasing trend suggested respectively by Kupfer and Reineck: the result is that the solution obtained is unacceptable since the tangential tension v_{cr} due to aggregate interlocking grows above the breaking tension of the concrete f'_c. This does not imply a limitation of the proposed method, but is due to the lack of suitable models capable of predicting the complex phenomenon of aggregate interlock accurately. At the moment there are no available formulations which can satisfactorily estimate the value of the tangential tension v_{cr} for variable loading because aggregate interlock is influenced by the irregular geometry of the fracture surface, by the expulsion of concrete fragments and by the high number of variables required to accurately define a phenomenon which is very difficult to quantify at an experimental stage.

8.1 Section n. 1

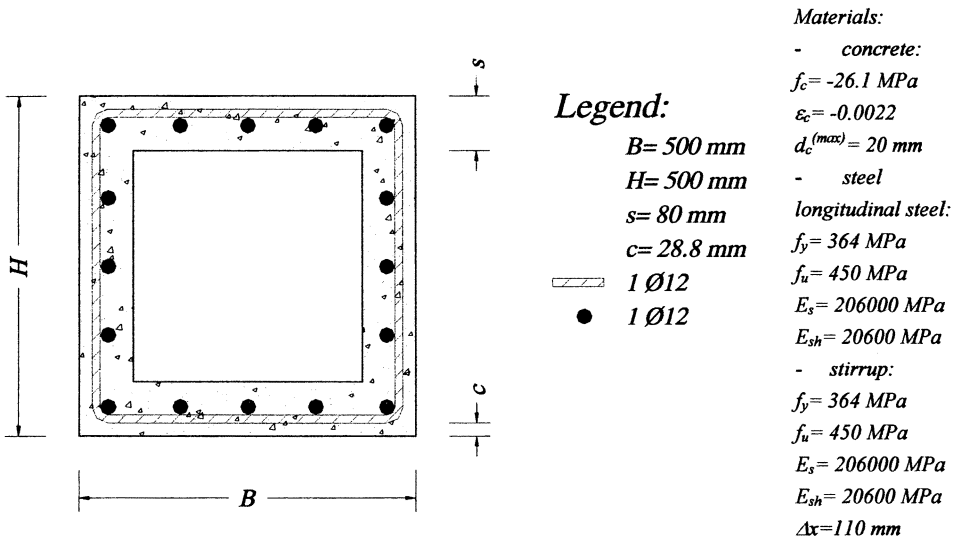

Fig. 12 Section n. 1

	A	*B*	*ω*	*φ*	$t_{in.}$	$t_{fin.}$	*n*
N [N]	0	0	0	0	0	0	0
M_x [Nmm]	70000	370000	1	0	0	15π	15
M_y [Nmm]	0	0	0	0	0	0	0
M_z [Nmm]	0	0	0	0	0	0	0

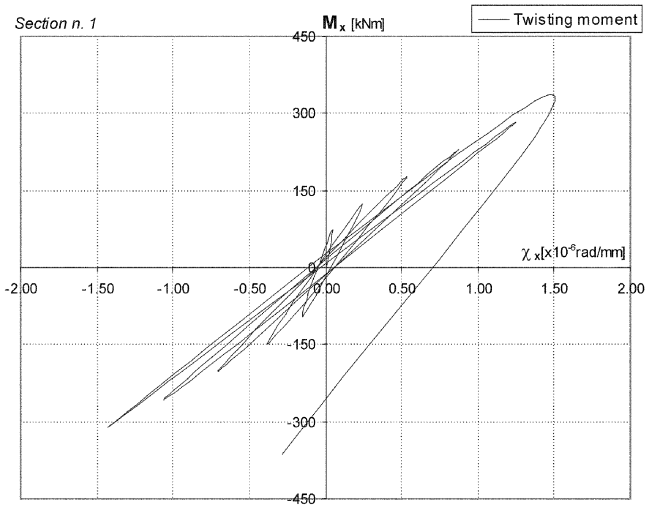

Fig. 13 Relation of the twisting moment-torsional curvature

	A	B	ω	φ	$t_{in.}$	$t_{fin.}$	n
N [N]	1000	26000	1	0	0	15π	15
M_x [Nmm]	60000	400000	1	0	0	15π	15
M_y [Nmm]	0	0	0	0	0	0	0
M_z [Nmm]	0	0	0	0	0	0	0

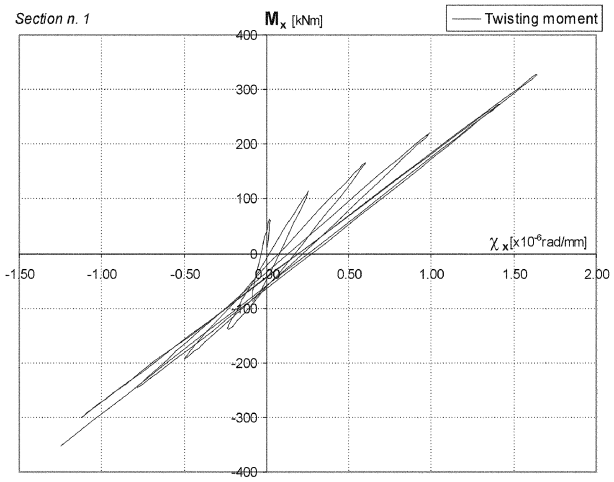

Fig. 14 Relation of the twisting moment-torsional curvature

	A	B	ω	φ	$t_{in.}$	$t_{fin.}$	n
N [N]	0	75000	1	0	0	15π	15
M_x [Nmm]	70000	270000	1	0	0	15π	15
M_y [Nmm]	0	100000	1	0	0	15π	15
M_z [Nmm]	0	0	0	0	0	0	0

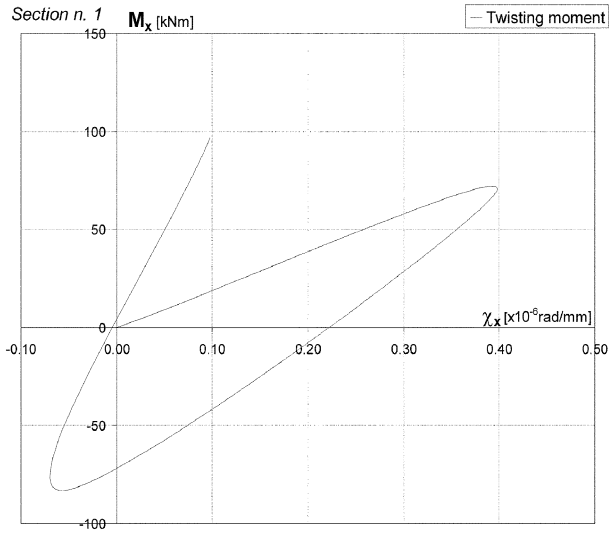

Fig. 15 Relation of the twisting moment-torsional curvature

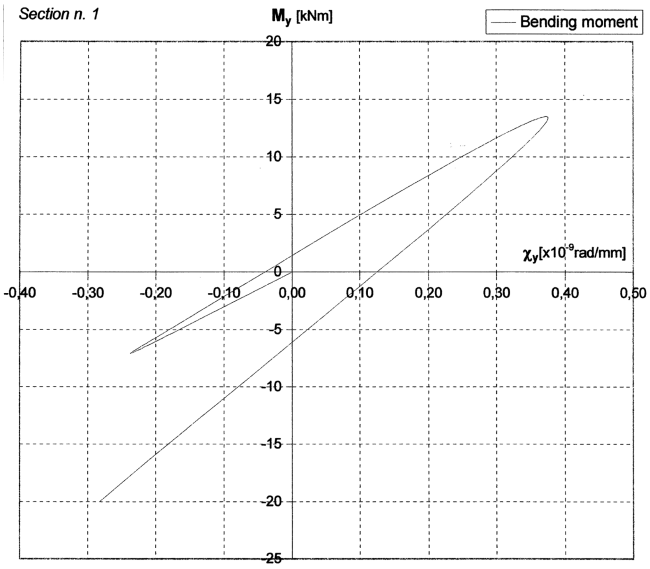

Fig. 16 Relation of the twisting moment-torsional curvature

8.2 Section n. 2

The numerical results obtained with the proposed procedure for a circular section beam similar to the beams used for bridge piers are illustrated in Fig. 18 while Fig. 17 shows the physical-geometrical characteristics of the sections analysed and the action-deformation curvatures.

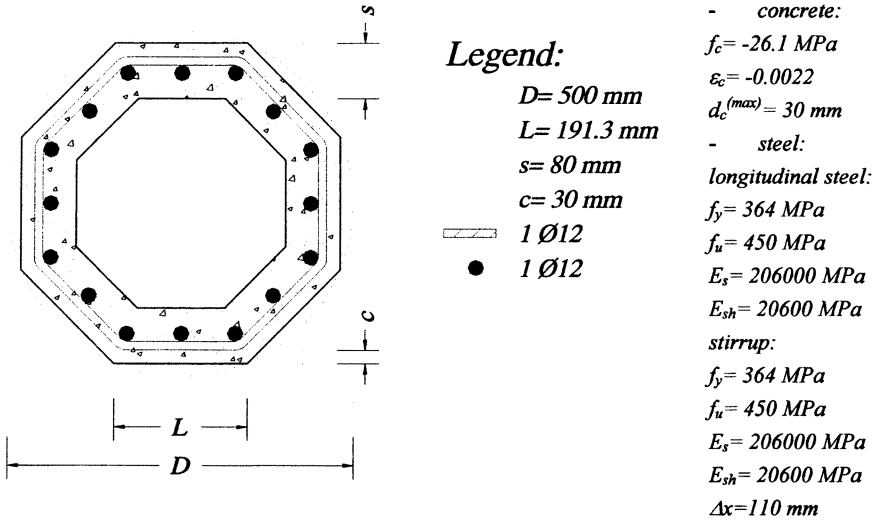

Fig. 17 Section n. 2

	A	*B*	ω	φ	$t_{in.}$	$t_{fin.}$	*n*
N [N]	0	0	0	0	0	0	0
M_x [Nmm]	60000	260000	1	0	0	12π	12
M_y [Nmm]	0	0	0	0	0	0	0
M_z [Nmm]	0	0	0	0	0	0	0

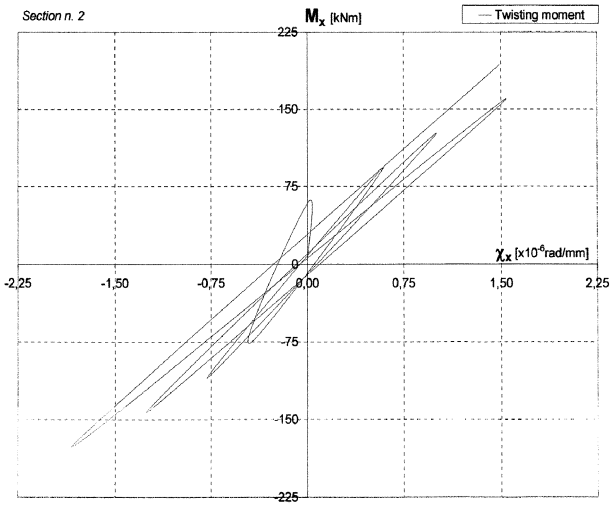

Fig. 18 Relation of the twisting moment-torsional curvature

	A	*B*	ω	φ	$t_{in.}$	$t_{fin.}$	*n*
N [N]	0	25000	1	0	0	12π	12
M_x [Nmm]	60000	660000	1	0	0	12π	12
M_y [Nmm]	0	10000	1	0	0	12π	12
M_z [Nmm]	0	0	0	0	0	0	0

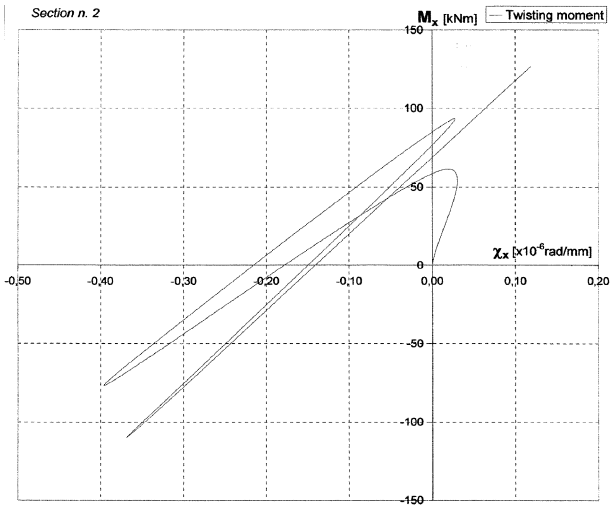

Fig. 19 Relation of the twisting moment-torsional curvature

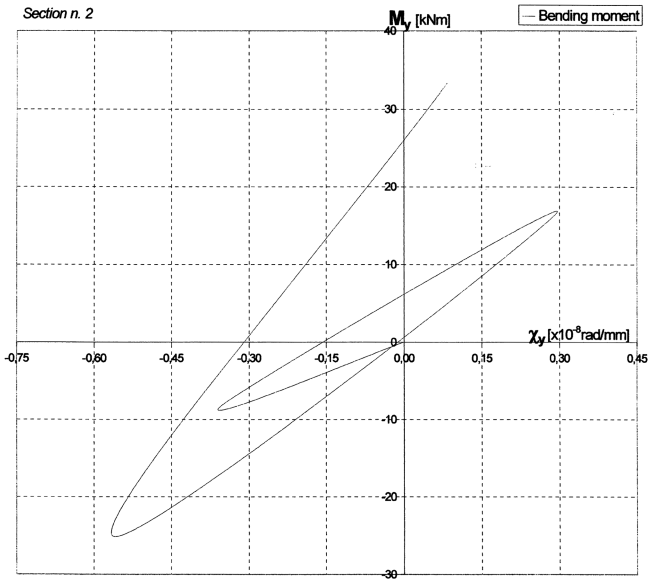

Fig. 20 Relation of the bending moment-flexional curvature

8.3 Section n. 3

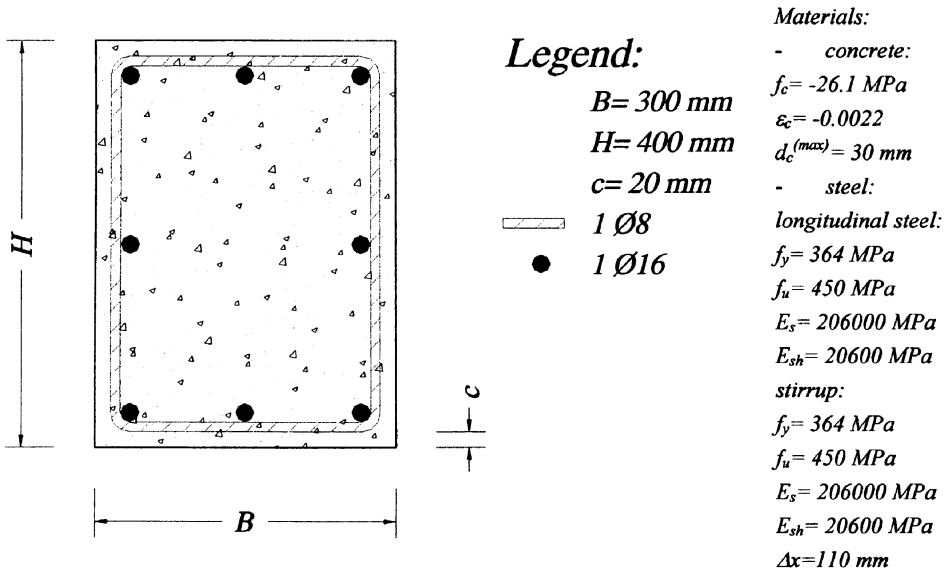

Fig. 21 Section n. 3

	A	B	ω	φ	$t_{in.}$	$t_{fin.}$	n
N [N]	0	0	0	0	0	0	0
M_x [Nmm]	25000	2122.065	1	0	0	15π	15
M_y [Nmm]	0	0	0	0	0	0	0
M_z [Nmm]	0	0	0	0	0	0	0

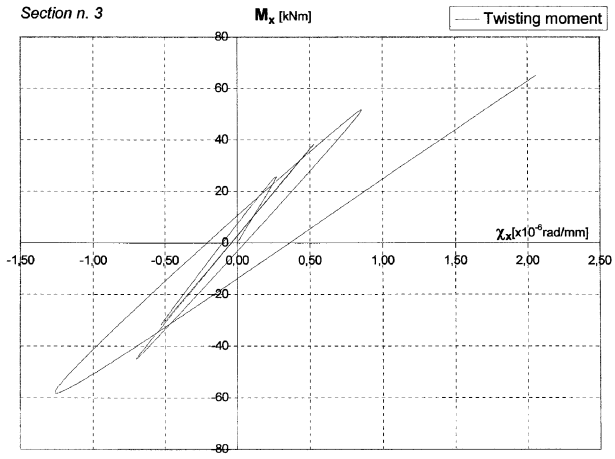

Fig. 22 Relation of the twisting moment-torsional curvature

	A	B	ω	φ	$t_{in.}$	$t_{fin.}$	n
N [N]	0	0	0	0	0	0	0
M_x [Nmm]	25000	2122.065	1	0	0	15π	15
M_y [Nmm]	0	7957.74	0	0	0	15π	15
M_z [Nmm]	0	0	0	0	0	0	0

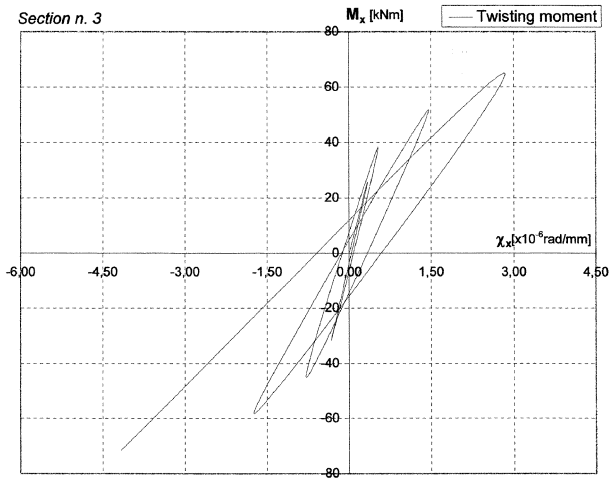

Fig. 23 Relation of the twisting moment-torsional curvature

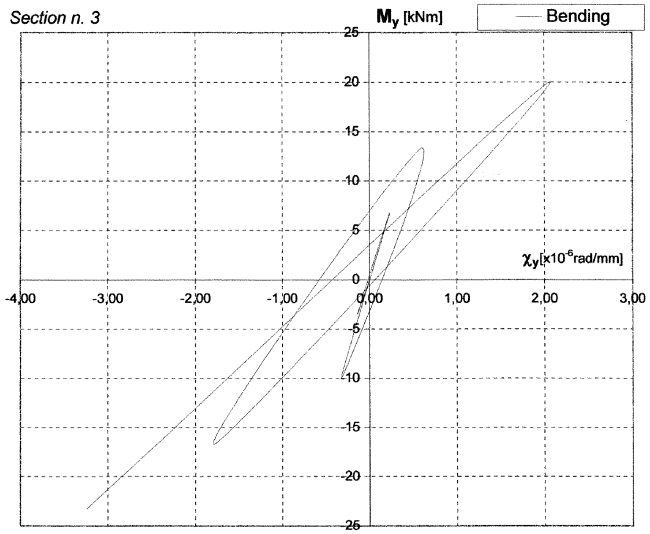

Fig. 24 Relation of the bending moment-flexional curvature

9. Conclusions

The aim of this work is to provide a numerical procedure for analysing the non linear dynamic behaviour of reinforced concrete beam elements under cyclical coupled torsion, biaxial flexure and axial loading conditions. In actual technical literature and codes theoretical and experimental studies are developed to predict only static or dynamic non linear behaviour, for uncoupled loading conditions, of reinforced beam elements. The damages find in framed reinforced structures subjected to recent earthquakes of high intensity emphasise a more realistic prediction of the three dimensional seismic force interaction in structural members. The procedure proposed in this paper, as an extension of the MCFT approach and as an improvement of the DSFM, realistically predict the non linear cyclical compression or tension fields in reinforced concrete beams and then may be a robust basis to further evaluate the global stiffness of three dimensional frames under medium or high seismic actions, according to a non linear dynamic F.E.M. approach. The numerical results obtained by means of the proposed procedure have shown that the influence of shear effects are nearly negligible and that the currently available experimental/theoretical formulations for cyclic loads give a not satisfactory estimate of the tangential critical tension owing to aggregate interlock. The computer procedure proposed may be a useful tool to check much more experimental results which shall be carried out on high strength reinforced concrete beams.

References

Ali, M.A. and White, R.N. (1999), "Enhanced contact model for shear friction of normal and high-strength concrete", *ACI Struct. J.*, May-June, 348-360.

Assa, B. and Nishiyama, M. (1998), "Prediction of load-displacement curve of high-strength concrete columns under simulated seismic loading", *ACI Struct. J.*, September-October, 547-557.

Bahn, B.Y. and Hsu, C.T.T. (2000), "Cyclically and biaxially loaded reinforced concrete slender columns", *ACI Struct. J.*, May-June, 444-454.
Bhide, S.B. and Collins, M.P. (1989), "Influence of axial tension on the shear capacity of reinforced concrete members", *ACI Struct. J.*, September-October, 570-581.
Cocchi, G.M. and Volpi, M. (1996), "Inelastic analysis of reinforced concrete beams subjected to combined torsion", *Comput. Struct.*, **61**(3), 479-494.
Duthinh, D. (1999), "Sensitivity of shear strength of reinforced concrete and prestressed concrete softening according to modified compression", *ACI Struct. J.*, July-August, 495-508.
Elmosieri, M., Kianoush, M. and Tso, W.K. (1998), "Nonlinear analysis of cyclically loaded reinforced concrete structures", *ACI Struct. J.*, November-December, 725-739.
Gambarova, P.G. (1987), "Modelling of interface problems in reinforced concrete", IABSE Colloquium Delft, 1-16.
Hsu, T.T.C. and Mo, Y.L. (1985), "Softening of concrete in torsional members-theory and tests", *ACI J.*, May-June, 290-303.
Hsu, T.T.C. and Zhang, L.X.B. (1997), "Nonlinear analysis of membrane elements by fixed-angle softened-truss model", *ACI Struct. J.*, September-October, 483-492.
Leung, M.B. and Schnobrich, W.S. (1987), "Reinforced concrete beams subjected to bending and torsion", *J. Struct. Eng.*, ASCE, **113**(2), February, 307-321.
Morcos, S.S. and BJorhovede, R. (1995), "Fracture modelling of concrete and steel", *J. Struct. Eng.*, ASCE, July, 1125-1133.
Onsongo, W.M. (1978), "The diagonal compression field theory for reinforced concrete beams subjected to combinated torsion, flexural and axial load", PhD Thesis Presented to the University of Toronto, Toronto, Ontario, Canada.
Pang, X.D. and Hsu, T.T.C. (1996), "Fixed angle softened truss model for reinforced concrete", *ACI Struct. J.*, March-April, 197-207.
Paulay, T. and Loeber, P.J., "Shear transfer by aggregate interlock", Shear in reinforced Concrete Sp-42. American Concrete Institute, Farmington Hills, Mich., 1-15.
Vecchio, F.J. (1999), "Towards cyclic load modelling of reinforced concrete", *ACI Struct. J.*, March-April, 193-202.
Vecchio, F.J. (2000a), "Analysis of shear-critical reinforced concrete beams", *ACI Struct. J.*, January-February, 102-110.
Vecchio, F.J. (2000b), "Disturbed stress field model for reinforced concrete: formulation", *J. Struct. Eng.*, ASCE, September, 1070-1077.
Vecchio, F.J. and Collins, M.P. (1986), "The modified compression-field theory for reinforced concrete elements subjected to shear", *ACI Struct. J.*, March-April, 219-231.
Vlasov, V.Z., "Thin walled elastic bar", 2ª edizione, Fimatgiz, Mosca, 1959 (traduzione in inglese a cura di: Isdral program for scientific traslation, Gerusalemme, 1961).
Wagner, H. and Pretschner, W. (1936), "Torsion and buckling of open section", NACA Tech. Mem. N. 784.

Appendix: Determination of thickness t_{di} of the small elements of the equivalent hollow section

It has been observed (Onsongo 1978) that when a beam is subjected to twisting and bending actions, its external surface does not remain flat: the torsion curvature χ_x and the flexional curvatures χ_y and χ_z cause a deflection of the compressed strut of the equivalent space truss specified by the curvature χ_n, orthogonal to the direction of the strut, if the fibres of the external surface are compressed.

Consider the small wall element, in which the local frame of reference *x-s* is indicated respectively in longitudinal and transversal directions, the origin O' and the compressed diagonal along the line AB, inclined by θ with respect to the longitudinal direction. The deformation of the surface O'ABC, due to the twisting action, can be expressed by the equation:

$$w_{tor.} = \chi_x xs \tag{A1}$$

describing a hyperbolic paraboloid and the flexional contribution to deformation, given by the equation:

$$w_{fles.} = \frac{1}{2}\chi_s x^2 \tag{A2}$$

that defines a parabolic cylinder having axis *s*.

In conclusion the deformed surface O'ABC, can be expressed by the contribution of the two terms:

$$w = w_{tor.} + w_{fles.} = \chi_x xs + \frac{1}{2}\chi_s x^2 \tag{A3}$$

Deriving this expression with respect to the direction *m* of the compressed strut, we have:

$$\frac{\partial w}{\partial m} = \frac{\partial w}{\partial x}\cdot\frac{\partial x}{\partial m} + \frac{\partial w}{\partial s}\cdot\frac{\partial s}{\partial m} = (\chi_x s + \chi_s x)\cos\theta + \chi_x x\sin\theta \tag{A4}$$

The curvature of the strut can be approximated with the second derivate:

$$\chi_n = \frac{\dfrac{\partial^2 w}{\partial m^2}}{\pm\left[1 + \left(\dfrac{\partial w}{\partial m}\right)^2\right]^{\frac{3}{2}}} \cong \frac{\partial^2 w}{\partial m^2} = \frac{\partial}{\partial x}\left(\frac{\partial w}{\partial m}\right)\cdot\frac{\partial x}{\partial m} + \frac{\partial}{\partial s}\left(\frac{\partial w}{\partial m}\right)\cdot\frac{\partial s}{\partial m} \tag{A5}$$

and after derivation, we have:

$$\chi_n \cong \frac{\partial^2 w}{\partial m^2} = (\chi_s\cos\theta + \chi_x\sin\theta)\cos\theta + \chi_x\sin\theta\cos\theta \tag{A6}$$

in conclusion:

$$\chi_n = \chi_s\cos^2\theta + 2\chi_x\sin\theta\cos\theta \tag{A7}$$

$$\chi_s = \chi_y\sin\varphi - \chi_z\cos\varphi \tag{A8}$$

Introducing (A8) in (A7) we obtain the equation expressing the curvature of the concrete strut according to the flexural and twisting curvatures:

$$\chi_n = (\chi_y\sin\varphi - \chi_z\cos\varphi)\cos^2\theta + \chi_x\sin(2\theta) \tag{A9}$$

This congruence equation permits evaluating the thickness of the compressed diagonal since, due to curvature χ_n, the deformation of the compressed strut varies through the thickness t_d of the strut.

Experimental tests (Onsongo 1978) demonstrate the validity of the hypothesis that considers a linear development of the average principal compression deformation along the thickness, with maximum value on the external surface ε_{ds}, and null value in correspondence of the thickness t_d, that in this way becomes the effective thickness of the compressed diagonal.

The thickness can be evaluated as follows:

$$t_d = -\frac{\varepsilon_{ds}}{\chi_n} \tag{A10}$$

In the behaviour of the space truss, due to deflection of the diagonal, a certain portion of the section is

subjected to traction and is ignored, while the part under compression is effectively considered as resistant to the stresses applied.

Indicating with ε_d the deformation situated half way up the thickness, we have:

$$\varepsilon_{ds} = 2 \cdot \varepsilon_d \tag{A11}$$

Considering the above, through equation (A10) the thickness of the hollow section is an equivalent thickness in the model adopted, bearing in mind that due to the presence of biaxial flexure in addition to torsion and axial forces, such thickness is variable along the edge of the section.

In the case of a hollow section having a given thickness $t_d^{(\max)}$, maintaining the hypothesis of linear variations through the thickness of the compression deformations and, if the thickness thus calculated with (A10) is greater than the maximum $t_d^{(\max)}$, the following condition is assumed:

$$t_d = t_d^{(\max)} \tag{A12}$$

Notation

z_{Pi} ; y_{Pi} : coordinates of the prime extremum of the side of the small element in the principal frame of reference of the given section;

z_{Pi+1} ; y_{Pi+1} : coordinates of the second extremum of the side of the small element in the principal frame of reference of the given section;

t_d : thickness of the compressed strut;

φ_l : anomaly of the side of the given section containing the segment $P_i\ P_{i+1}$ corresponding to first side of the small element;

z_{si} ; y_{si} : coordinates of the point of application of the resultant of σ_l acting on small element $\underline{\boldsymbol{x}}_i$;

z_{ci} ; y_{ci} : coordinates of the barycentre of the small element in the principal frame of reference of the given section;

ρ_{sl} : percentage of reinforcement in longitudinal direction;

ρ_{st} : percentage of reinforcement in transversal direction;

f_{sl} : average tension on the longitudinal reinforcements;

f_{st} : average tension on the transversal reinforcements;

f_{c1} : average principal traction tension on concrete due to the steel-concrete adherence;

f_{c2} : average principal compression tension on concrete;

f_{slcr} : punctual tension on longitudinal reinforcements in proximity of the crack;

f_{stcr} : punctual tension on transversal reinforcements in proximity of the crack;

v_{cr} : tangential tension developed at the cracking interface;

A_l : longitudinal reinforcement area;

B : basis of the small element;

A_t : transversal reinforcement area (stirrups);

Δx : spacing between the transversal reinforcements (stirrups);

q : flow due to the transversal tensions;

n : number of small elements subdividing the section;

A_i : area of the small element $\underline{\boldsymbol{x}}_i$;

A_{sj} : area of the reinforcement $\underline{\boldsymbol{x}}_j$;

m : total number of longitudinal reinforcements in the section;

z_{si} : abscissa of the centre of the longitudinal reinforcement $\underline{\boldsymbol{x}}_j$;

$\underline{r}_i$: vector ray of the resultant of the tangential tensions;

$\underline{z}$: axis z unit vector;

$\underline{y}$: axis y unit vector;

ε_1 : total deformation in direction 1;

ε_2 : total deformation in direction 2;

γ_{12} : total shear deformation associated to the directions 1-2;
ε_l : total or apparent deformation in direction *l*;
ε_t : total or apparent deformation in direction *t*;
γ_{lt} : total or apparent shear deformation in direction *l*-*t*;
ε_{c1} : net deformation in direction 1;
ε_{c2} : net deformation in direction 2;
γ_{c12} : net shear deformation associated to the directions 1-2;
σ_1 : principal traction tension;
σ_2 : principal compression tension;
τ_{12} : tangential tension in the principal frame of reference;
σ_l : tension in direction *l*;
σ_t : tension in direction *t*;
τ_{lt} : tangential tension in the frame of reference *l*-*t*;
θ_ε : inclination angle of the principal directions of total deformation;
θ_σ : inclination angle of the principal directions of net deformation;
θ : inclination angle of the cracks coinciding with θ_σ;
c_l : maximum distance from the longitudinal reinforcements, measured perpendicularly to the bars;
c_t : maximum distance from the transversal reinforcements, measured perpendicularly to the bars;
s_l : spacing between the longitudinal reinforcements;
s_t : spacing between the transversal reinforcements;
d_{bl} : diameter of the longitudinal reinforcements;
d_{bt} : diameter of the transversal reinforcements;
ρ_l : spacing between the longitudinal reinforcements;
ρ_t : spacing between the transversal reinforcements;
$\underline{\varepsilon}^c$: net deformations vector;
$\underline{\varepsilon}^s$: vector of deformations due to slippage;
$\underline{\varepsilon}^0$: vector of elastic deformations or connected to these such as thermal jumps, Poisson effect, aggregated alkali, etc.;
$\underline{\varepsilon}^p$: plastic deformations vector;
ε^0_{sl} : possible deformation impressed on the reinforcement in direction *l* (for effect of pre-tensioning);
ε^0_{st} : possible deformation impressed on the reinforcement in direction *t* (for effect of pre-tensioning);
w : width of the crack;
δ_s : relative slippage between the cracks;
s : spacing between the cracks;
$\Delta\varepsilon_1$: increase of the reinforcements deformation in correspondence of the cracks;
$\underline{\Delta\gamma}_{12}$: increase of the slippage deformation correspondence of the cracks;
$\overline{ab}$: distance between point *a* and point *b* Fig. 6(b);
$\gamma_{lt}^{(A)}$: tangential deformation of small element A;
$\gamma_{lt}^{(B)}$: tangential deformation of small element B;
$\varepsilon_l^{(A)}$: longitudinal deformation of small element A;
$\varepsilon_l^{(B)}$: longitudinal deformation of small element B;
L_e : external work;
L_i : internal work;
N : axial force;
η : axial deformation;
M_x : twisting moment;
χ_x : torsional curvature;
M_y : bending moment in direction *y*;
χ_y : flexing curvature due to M_y;
M_z : bending moment in direction *z*;
χ_z : flexing curvature due to M_z;
ε_0 : deformation corresponding to maximum uniaxial compression in concrete;

f_p : maximum compression tension in concrete (peak tension);
ε_p : corresponding deformation f_p (peak deformation);
f_{c1} : traction tension in concrete;
f_{c2} : reduced compression tension in cracked concrete;
f'_{c2} : compression tension in cracked concrete comprehensive of the softening effect;
E_c : tensile module of the concrete tangent at the source;
ε_{c1} : traction deformation of concrete;
ε_{cr} : correspondent deformation to the start of cracking;
f'_t : maximum traction tension in non cracked concrete;
f'_c : maximum compression tension in non cracked concrete (obtained with a test on a cylindrical sample);
$f_{c1}^{(stiff.)}$: traction tension in concrete associated to "tension stiffening";
c_t : coefficient of "tension stiffening";
d_b : diameter of the bars;
ε_{cm} : maximum compression deformation obtained during the previous loading in the direction in question;
f_{cm} : tension corresponding to ε_{cm};
ε_c^p : plastic deformation;
$f_{bc}(\varepsilon_c)$: tension calculated on the base curve in correspondence of ε_c;
ε_p : deformation correspondent to peak tension of the curve envelope;
ε_c^p : plastic deformation;
$\varepsilon_c^{p'}$: instantaneous plastic deformation corresponding to deformation ε_c;
f_{cm} : tension corresponding to ε_{cm};
ε_{cm} : maximum compression deformation reached during the previous loading in the direction in question;
E_{cm} : tensile module of unloading;
$f_c(\varepsilon_c)$: unloading tension corresponding to deformation ε_c;
ε_{tm} : maximum traction deformation obtained during the previous loading;
ε_t^p : plastic deformation;
f_{tm} : tension corresponding to ε_{tm};
$f_{bt}(\varepsilon_t)$: tension calculated on the base curve for a deformation equal to ε_t;
R_0 : 20;
a_1 : 18.5;
a_2 : 0.0015;
f_y : yield stress;
ε_y : deformation corresponding to start of yielding;
E_0 : tensile module tangent in source;
E_1 : tensile module of positive strain hardening;
b : E_1/E_0;
σ_0 : tension corresponding to the point of intersection of the asymptotes;
ε_0 : deformation corresponding to the point of intersection of the asymptotes;
σ_r : tension corresponding to the point reached in the previous cycle;
ε_r : deformation corresponding to the point reached in the previous cycle;
ξ : deformation corresponding to the deformation difference between the intersection point of the asymptotes and the point of minimum or maximum deformation previously reached;
c : aggregate maximum dimension [mm];
σ : tension acting orthogonally to the crack [MPa];
ε_{ds} : maximum deformation of the strut in proximity of the edge of the section;
$N(t)$: axial stress function of the temporal variable;
$N_{cal.}$: calculated axial stress;
$M_x(t)$: twisting moment function of the temporal variable;
$M_{x\ cal.}$: calculated twisting moment;

$M_y(t)$: bending moment in direction y function of the temporal variable;
$M_{y\ cal.}$: bending moment in direction y calculated;
$M_z(t)$: bending moment in direction z function of the temporal variable;
$M_{z\ cal.}$: bending moment in direction z calculated;
χ_n : curvature of the strut.